



HAL
open science

Relative Sea Level and Abrupt Mass Unloading in Barbados during the Holocene

Julien Gargani

► **To cite this version:**

Julien Gargani. Relative Sea Level and Abrupt Mass Unloading in Barbados during the Holocene. *Geomorphology*, 2022, 413, pp.108353. <10.1016/j.geomorph.2022.108353>. <hal-03723465>

HAL Id: hal-03723465

<https://hal.science/hal-03723465v1>

Submitted on 18 Aug 2022

HAL is a multi-disciplinary open access archive for the deposit and dissemination of scientific research documents, whether they are published or not. The documents may come from teaching and research institutions in France or abroad, or from public or private research centers.

L'archive ouverte pluridisciplinaire **HAL**, est destinée au dépôt et à la diffusion de documents scientifiques de niveau recherche, publiés ou non, émanant des établissements d'enseignement et de recherche français ou étrangers, des laboratoires publics ou privés.



HAL Authorization

Abrupt Mass Unloading and Relative Sea Level in Barbados during the Holocene

Julien Gargani^{1,2}

¹Université Paris-Saclay, CNRS, Geops, Orsay, France.

²Université Paris-Saclay, Centre d'Alembert, Orsay, France.

Highlight

- An abrupt mass unloading of $30 \pm 10 \text{ km}^3$ occurred in Barbados and caused isostatic adjustment of $0.45 \pm 0.15 \text{ mm/yr}$.
- An uplift increases from 0.34 to 0.8 mm/yr at $11.2 \pm 0.1 \text{ kyr BP}$ in less than 0.2 kyr explain coral reef elevation in Barbados.
- 150 yr after the termination of Younger Drias and 300 yr before the abrupt mass unloading, a sea-level drop of 4.8 m occurred, corresponding to meltwater pulse MWP-1B.

Abstract

Coral reef records sea-level as well as vertical movement. In Barbados, uplift variation is necessary to interpret one of the most complete coral reef record. Here we show that an abrupt mass unloading of $30 \pm 10 \text{ km}^3$ caused an uplift variation of $\sim 0.45 \pm 0.15 \text{ mm/yr}$ using a modelling approach. Simulations have been conducted for different volumes and elastic thicknesses. Isostatic adjustment in relation with an abrupt mass unloading explain the observed uplift rate increase from 0.34 mm/yr to 0.8 mm/yr that occurred 11.2 kyr ago. The reconstructed sea-level curve highlight a sea-level drop of 4.8 m drop, with a delay of 150 yr from the termination of Younger Dryas cold event and 300 yr before the abrupt mass unloading. This sea-level drop corresponds to meltwater pulse MWP-1B and is not an artefact. A stagnation of 500 yr occurred from 12 to 11.5 kyr BP. Relative sea level records are useful to detect past landslides and erosion. Accurate analysis and reconstruction of sea-level permit to determine sea-level drop caused by warming during the last thousand years.

30

31 **Keywords** : uplift; sea level; coral reef; isostasy; meltwater pulse; landslide

32 **1 Introduction**

33 Rapid sea-level rise could be better understood studying ongoing changes in the
34 climate system (Edwards et al., 2021; Hoojer and Vernimmen, 2021) and by studying the
35 abrupt sea-level changes that occurred in the past (Gargani and Rigollet, 2007; Bard et al.,
36 2010). Reconstruction of sea level could be based on well log and stratigraphic analysis (Haq
37 and Schutter, 2008), seismic and geomorphological observations (Bache et al., 2015) or coral
38 reef studies (Mesolella, 1967; Fairbank, 1989).

39 Reconstruction of sea level from coral reef must take into account tectonic movement
40 (Radtke and Schellmann, 2006; Peltier and Fairbank, 2006), glacio-hydro isostasy
41 (Austermann et al., 2013) and uncertainty associated with coral reefs species (Bard et al.,
42 2016). Isostatic adjustment could be also caused by erosion (Gargani, 2004) and landslide
43 (Smith and Wessel, 2000). Coastal erosion is underestimated (Regard et al., 2022) and coastal
44 as well as marine landslides are numerous (Urgeles and Camerlinghi, 2013). Consequently,
45 unloading processes on coastal vertical movement must be evaluate for accurate
46 reconstruction of relative sea level curves.

47 Accurate reconstruction of relative sea level curves is of fundamental importance due
48 to the numerous applications of these data. Relative sea level reconstruction could be used to
49 determine local paleogeography (Zinke et al., 2003), to estimate regional vertical movements
50 by comparing with a reference's sea level curve (Camoin et al., 2004; Pedoja et al., 2014) and
51 to discuss paleoclimate variation (Fairbank, 1989; Blanchon and Shaw, 1995).

52 The most complete record of sea-level is based on coral reef drilled at Barbados. Coral
53 reef record in Barbados is studied since several decades (Mesolella et al., 1969; Bender et al.,
54 1979). This record was used to calibrate relative sea level during the last 500 kyr (Bard et al.,
55 1990, Bard et al., 1990b; Gallup et al., 1994; Peltier and Fairbank, 2006; Abdul et al., 2016)
56 as well as to determine local uplift (Radtke and Schellmann, 2006).

57 In this study, the role of an abrupt mass unloading in the Tertiary terrain of the
58 Scotland District in the northeast of Barbados is investigated to estimates the potential uplift
59 change of coral reef located in the southwest of the island, near Bridgetown (Figure 1), from
60 14 to 9 kyr Before Present (BP). More fundamentally, the new sea level reconstruction

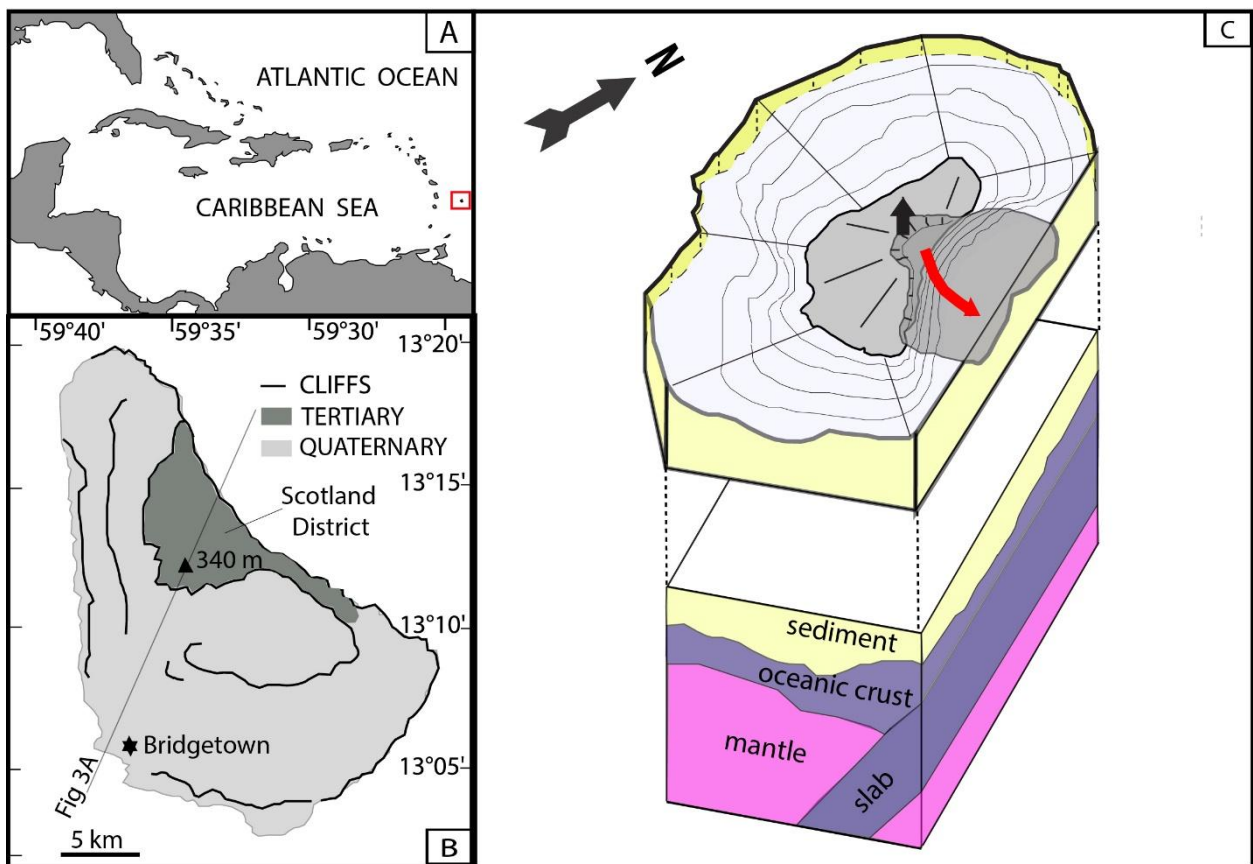
61 proposed in this study will be used to quantify the meltwater pulse MWP-1B (age, duration,
62 amplitude).

63

64

65 2 Geological context

66 Barbados Island (430 km²) lies on an accretionary prism above the subducting Atlantic
67 lithosphere that passes beneath the crust of the Caribbean plate (Westbrook et al.,
68 1988)(Figure 1). Deformed Tertiary sedimentary rocks are located below an uplifted
69 Quaternary reef-related cover (Speed, 1981) with a maximum age of 500-600 kyrs (Radtke
70 and Schellmann, 2006). The cause of passive uplift of sedimentary layers could be due to
71 compressive tectonic at the plate junction, mud diapirism or shale movements in deep
72 overpressured zones (Deville et al., 2006).

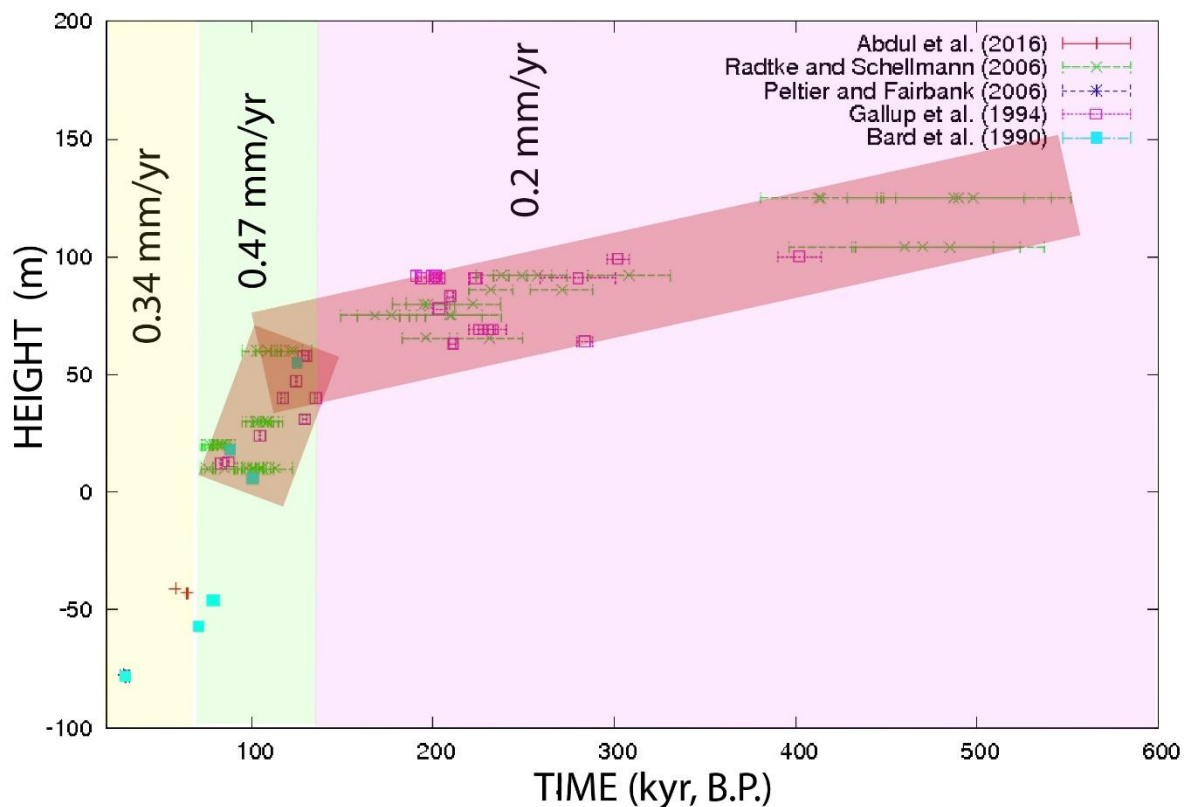


74

74 **FIGURE 1: Geographic and geological context. (A) Location of Barbados Island in the red**
75 **square, (B) Geological map of Barbados Island, (C) Schematic representation of mass**
76 **unloading and lithosphere geometry.**

77

78 Uplift rate in Barbados was not constant during the last 500 kyr (Radtke and
79 Schellmann, 2006) (Figure 2). From 200 to 500 kyr, uplift rate was around 0.2 mm/yr whereas
80 from 100 to 120 kyr ago, mean uplift rate was estimated to be of 0.47 ± 0.02 mm/yr (Radtke
81 and Schellmann, 2006). From 35 to 11.2 kyr BP, an uplift rate of 0.34 mm/yr is often assumed
82 (Peltier and Fairbank, 2006; Abdul et al., 2016). This uplift rate of 0.34 mm/yr was caused by
83 tectonic compression or diapirism (Speed, 1981; Westbrook et al., 1988; Bard et al., 2016).



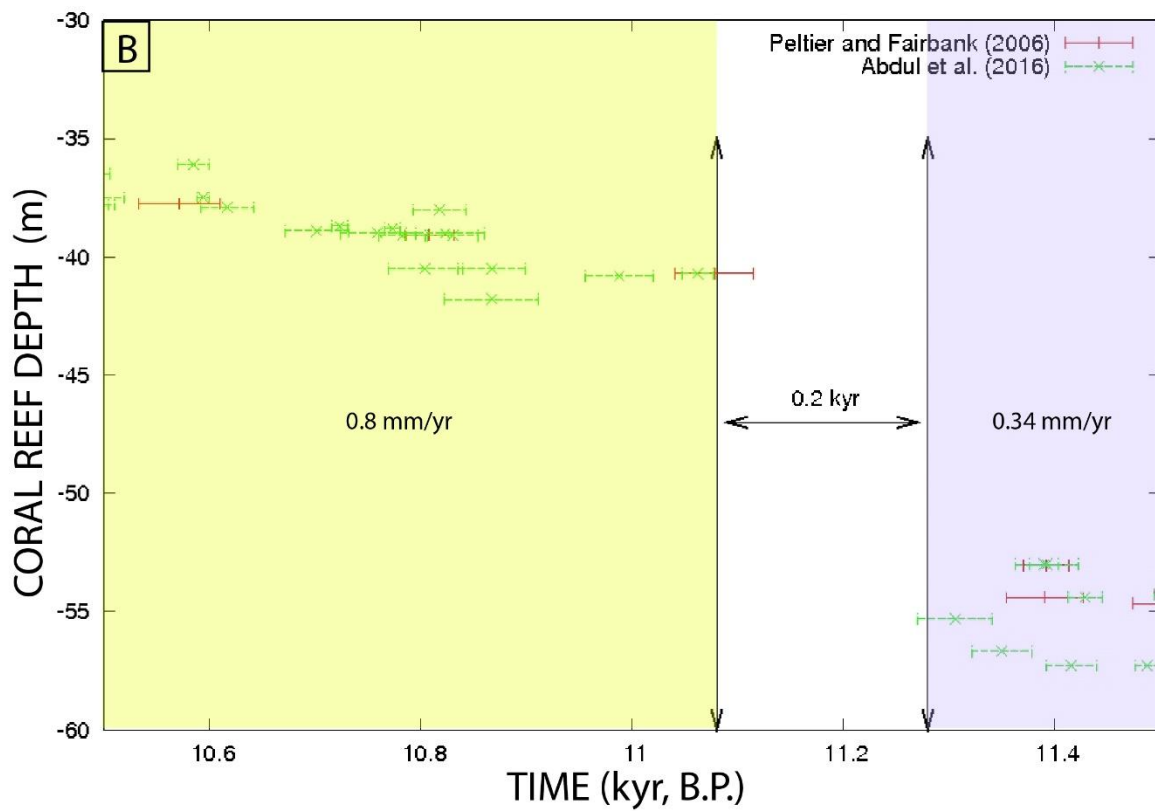
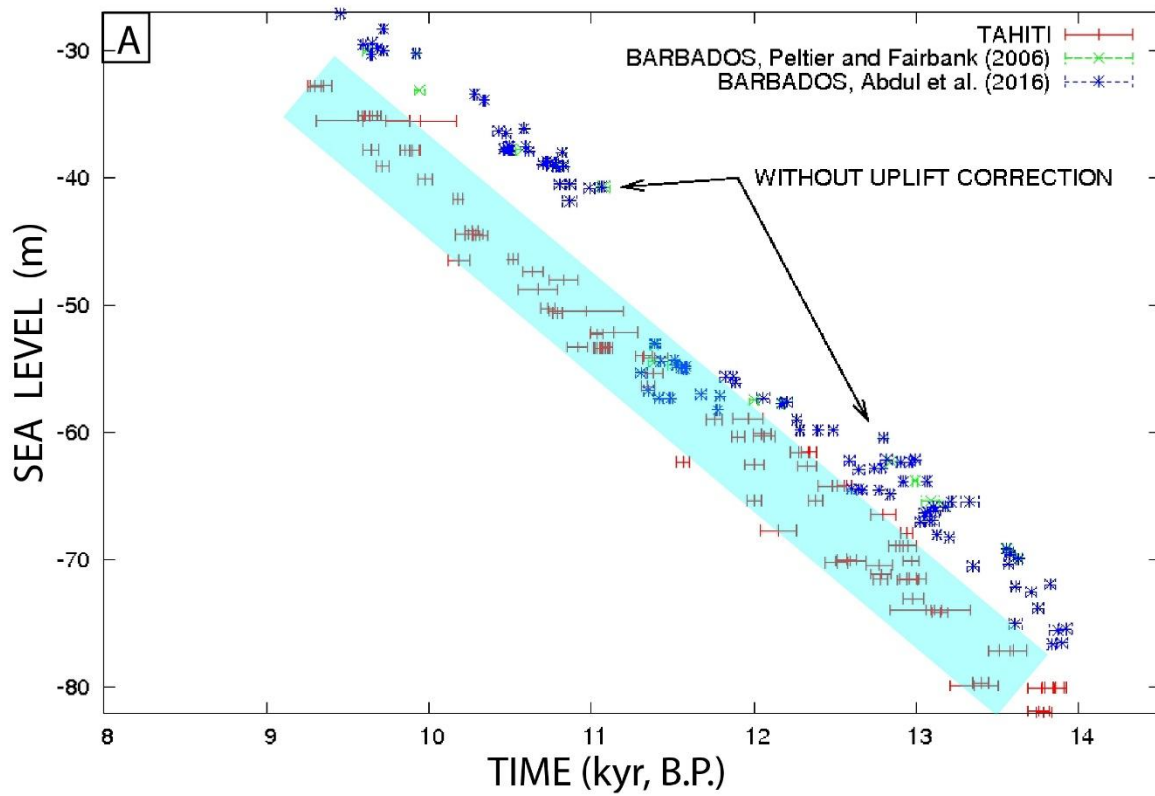
84

85 **FIGURE 2: Coral reef elevation and uplift. (A) Height of coral reefs in Barbados with ages**
86 **ranging from 20 to 600 kyrs (Bard et al., 1990b; Gallup et al., 1994; Peltier and Fairbank,**
87 **2006; Radtke and Schellmann, 2006; Abdul et al., 2016) and uplift rates.**

88 Without taking into account uplift correction, Barbados coral reefs have a significant
89 offset from sea-level reconstruction suggesting the existence of an uplift (Peltier and
90 Fairbank, 2006; Radtke and Schellmann, 2006; Abdul et al., 2016). The observed vertical
91 shift from sea-level curve range from 10 ± 2 m at 10.5 kyr to 4 ± 1 m at 13 kyr (Figure 3). At
92 11.2 kyr BP, there is less data during around 200 yr.

93 Recently, it was highlighted that there were several meters of offset between coral
94 reefs younger than 11.2 kyr and those older than 11.2 kyr (Abdul et al., 2016). This variation
95 of altitude was first attributed to a meltwater pulse record (MWP-1B) (Abdul et al., 2016;
96 Bard et al., 1996), but this offset was discarded by comparing with sea-level curves
97 established in other places (Bard et al., 2016; Lambeck et al., 2014; Carlson and Clark, 2012).
98 This shift was believed to occur 0.4 kyr after the end of Young Dryas (Abdul et al., 2016) that
99 finished 11.610 ± 40 kyr BP (Cheng et al., 2020). Nevertheless, the possibility that an uplift
100 variation with time occurred from 14 to 9 kyr has not been studied in Barbados, in spite of
101 older uplift variations (Radtke and Schellmann, 2006).

102



103

104 **FIGURE 3: Coral reef elevation and uplift. (A)** Sea level estimated from Tahiti coral
 105 reefs corrected from subsidence (0.25 mm/yr) in red compared with Barbados coral

106 reefs, without uplift correction, between 9 and 14 kyr B.P. in blue (Abdul et al., 2016)
107 and green (Peltier and Fairbank, 2006). Data for Tahiti (Bard et al., 2010) and for
108 Barbados (Peltier and Fairbank, 2006; Abdul et al., 2016) are only those of *Acropora*
109 *palmata* for clarity. (B) Coral reef elevation vs age from 11.5 to 10.5 kyr before present.
110 No uplift correction. The transition duration from the uplift rate of 0.34 mm/yr to 0.8
111 mm/yr is of 0.2 kyr and occurred from 11.28 to 11.08 kyr BP. Data are from Peltier and
112 Fairbank (2006) and Abdul et al. (2016).

113 In the Northeast part of the island, the absence of Quaternary rocks on an area of ~60
114 km² suggests significant erosion or/and landsliding during the last 500-600 kyr. The volume
115 of missing material caused by erosion and/or landslides in the Scotland District is significant
116 (~10 km³). Furthermore, bathymetric data suggests that missing material extend offshore the
117 Scotland District. Landslides and erosion occurred in this area during the last centuries (Prior
118 and Ho, 1972; Cruden et al., 2014), and are documented deep offshore on the accretionary
119 prism (Pichot et al. 2016). Unloading associated with large landslides is able to generate
120 isostatic adjustment (Smith and Wessel, 2000). High amount of erosion also generates
121 isostatic adjustment (Gargani, 2004) which main observed features are uplift and
122 geomorphological transformations of the slope (Gargani et al., 2010).

123

124 **2 Methods**

125 2.1 Isostatic adjustment modelling

126 In this study, the role of abrupt mass unloading on uplift rate variation is investigated
127 for the period from 14 kyr to 9 kyr BP by modelling the isostatic adjustment. Isostatic
128 adjustment is considered as an additional cause of uplift and is the only process modelled
129 here. It must be added to the other mechanisms responsible of the preexisting 0.34 mm/yr of
130 uplift rate.

131 Different unloaded mass were simulated corresponding to various volume displaced.
132 Three different volumes were considered (3 km³, 10 km³, 50 km³). A maximum of 10 km³
133 could have been displaced from the Scotland District by erosion or landslides. Offshore,
134 erosional features are observed and suggests supplementary mass unloading. Such volumes
135 have been observed for a large variety of landslides or erosion. The estimation of the uplift
136 depends also from the flexural rigidity.

137 In the Scotland District, the uplift $w(x)$ can be obtained by solving the equation
138 $\nabla^2(D \cdot \nabla^2 w(x,y)) + (\rho_a - \rho_s)g \cdot w(x,y) = \rho_s g [z_{init}(x,y) - z(x,y)]$, where the rigidity is defined by D
139 $= ET_e^3 / [12(1 - \nu^2)]$, with ρ_a and ρ_s the densities of asthenosphere and sedimentary rock, g the
140 acceleration of gravity, $z_{init} - z$ the missing material thickness, E the Young's modulus, T_e the
141 effective elastic thickness, and ν the Poisson's ratio (Turcotte and Schubert, 2001). $\nu = 0.25$, ρ_a
142 $= 3179 \text{ kg/m}^3$, $\rho_s = 2800 \text{ kg/m}^3$, $E = 10^{10} \text{ Pa}$, $40 \text{ km} < T_e < 60 \text{ km}$.

143 The elastic thickness in the Barbados area is of $50 \pm 10 \text{ km}$ (Lambeck et al., 2014;
144 Jimenez-Diaz et al., 2014) corresponding to a flexural rigidity of around 10^{23} N.m^2 . Resulting
145 vertical motion rates are calculated considering a constant displacement, during 10 kyr after
146 the abrupt mass displacement, in agreement with the time necessary to relax the viscous
147 properties of the lithosphere of $10 \pm 5 \text{ kyr}$ after isostatic adjustment (Mitrovica et al., 2000;
148 Van der Wal et al., 2010).

149 To avoid any overestimation of the uplift, the mass balance has been respected by
150 loading a comparable mass on the model than material has been unloaded. The loading mass
151 is located offshore, 35 km at the northeast of Barbados. In case of erosion and turbidite flow,
152 this could overestimate the loading.

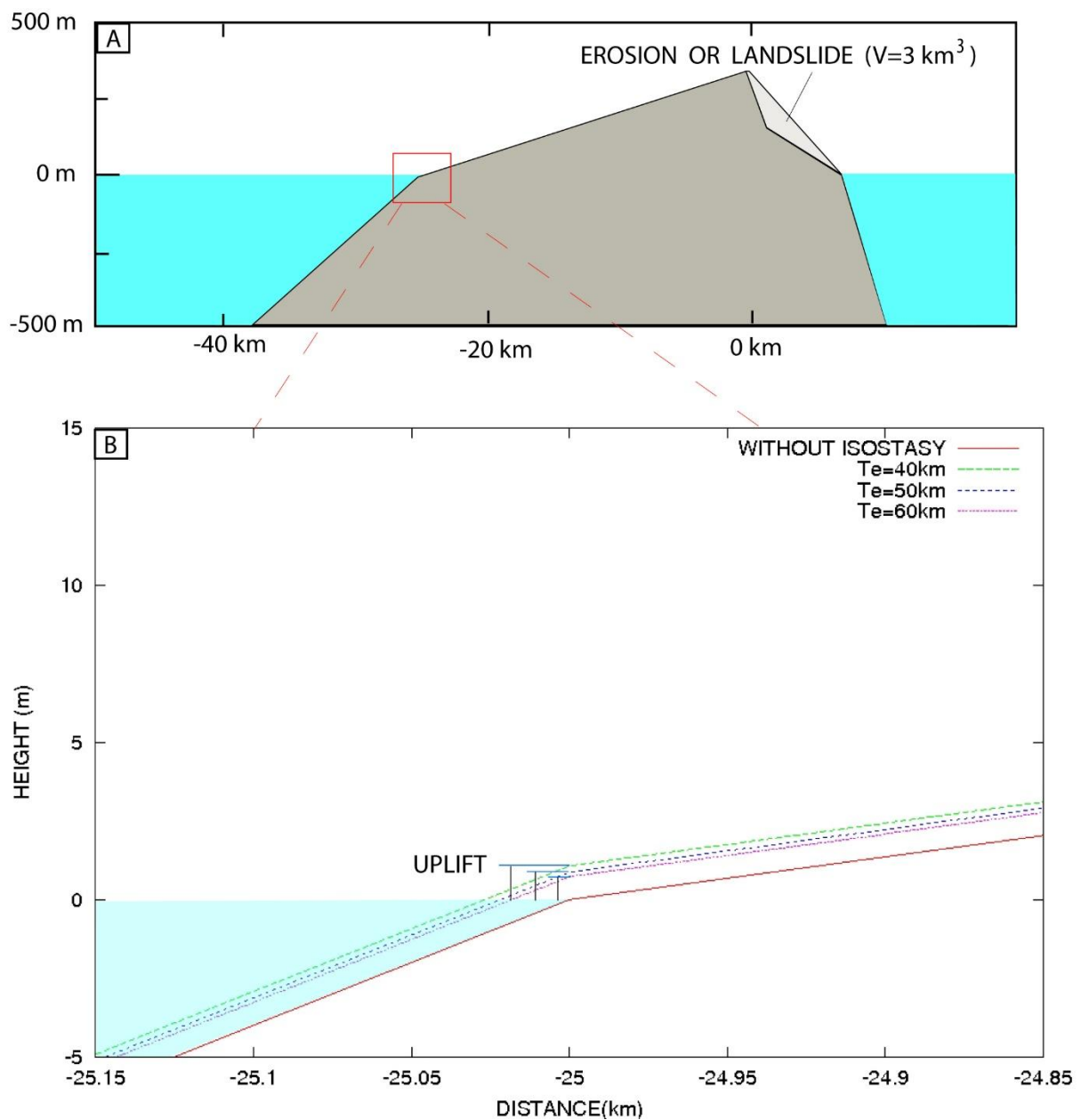
153 2.2 Comparison between modelled and observed uplift

154 In the present study, the modelling results concerning the uplift are compared with
155 observed data. In Barbados, coral reefs permit to evaluate relative sea level variation and local
156 vertical movement by comparing with a reference sea level curve. Barbados coral reef's data
157 used in this study were published by Abdul et al. (2016) and Peltier and Fairbank (2006). The
158 sea level curve considered as a reference is based on the data from Bard et al. (1990b, 1996,
159 2010). Only elevation obtained from *Acropora palmata* and U-Th are considered. Finally, a
160 new reference sea level curve is built using the reference sea level of Tahiti and the relative
161 sea-level curve of Barbados after correction of the uplift rate. Sea level trend from 14 to 9 kyr
162 BP, based on Barbados and Tahiti coral reef records corrected from uplift is described and
163 implication for meltwater pulse MWP-1B discussed.

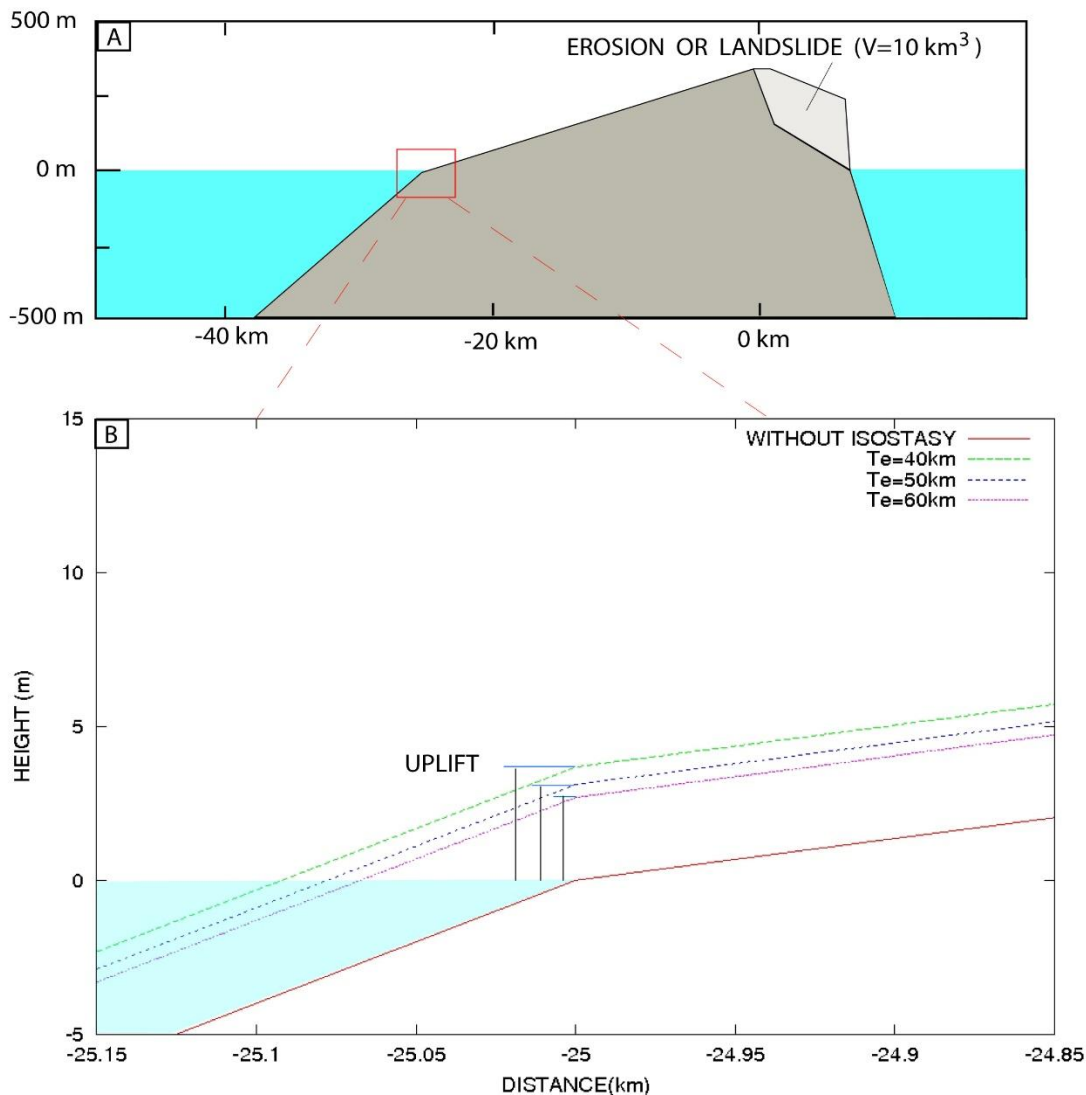
164 3 Results

165 Abrupt mass unloading, such as large erosion and landslide, causes an uplift through
166 an isostatic adjustment and impacted relative sea level variation. More precisely, the modelled
167 uplift is less than 2 m for an unloading of $8.4 \times 10^{12} \text{ kg}$, corresponding to a volume

168 displacement of 3 km^3 of sedimentary rocks (Figure 4). The modelled uplift after an abrupt
 169 mass unloading of 10 km^3 is of $3.25 \pm 0.75 \text{ m}$, depending on the elastic thickness of the
 170 lithosphere (Figure 5). When the mass unloading increases, the resulting uplift also increases.
 171 An abrupt mass unloading of 50 km^3 could cause an uplift of $6 \pm 1 \text{ m}$ (Figure 6A). The more
 172 the elastic thickness is, the less is the vertical displacement. The uplift caused by this process
 173 ranges from 3 to 6.5 m for a mass displacement of $20\text{-}40 \text{ km}^3$.



174
 175 **Figure 4: Isostatic adjustment after an abrupt mass unloading of 3 km^3 .** (A) Unloaded
 176 volume geometry, (B) Modelled uplift in the southwest part of the island after an abrupt
 177 mass unloading caused by an isostatic adjustment with elastic thicknesses of 40 km, 50
 178 km and 60 km.

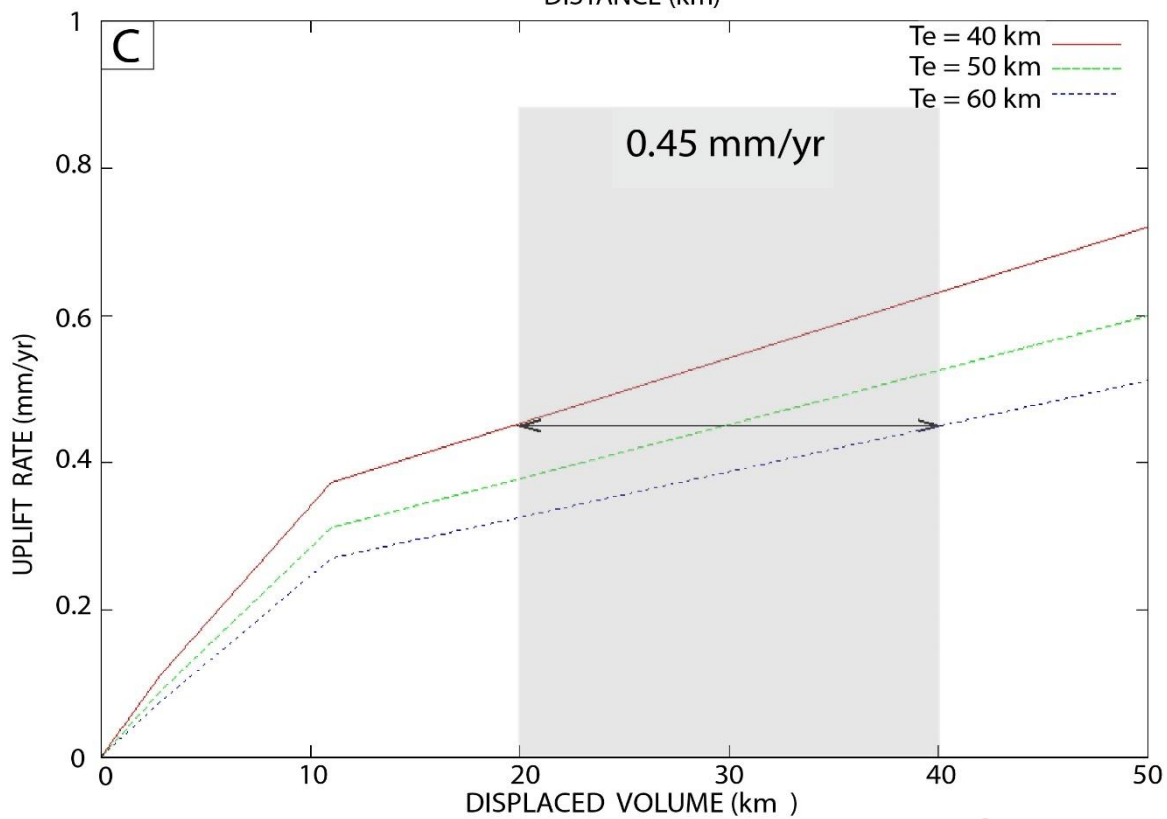
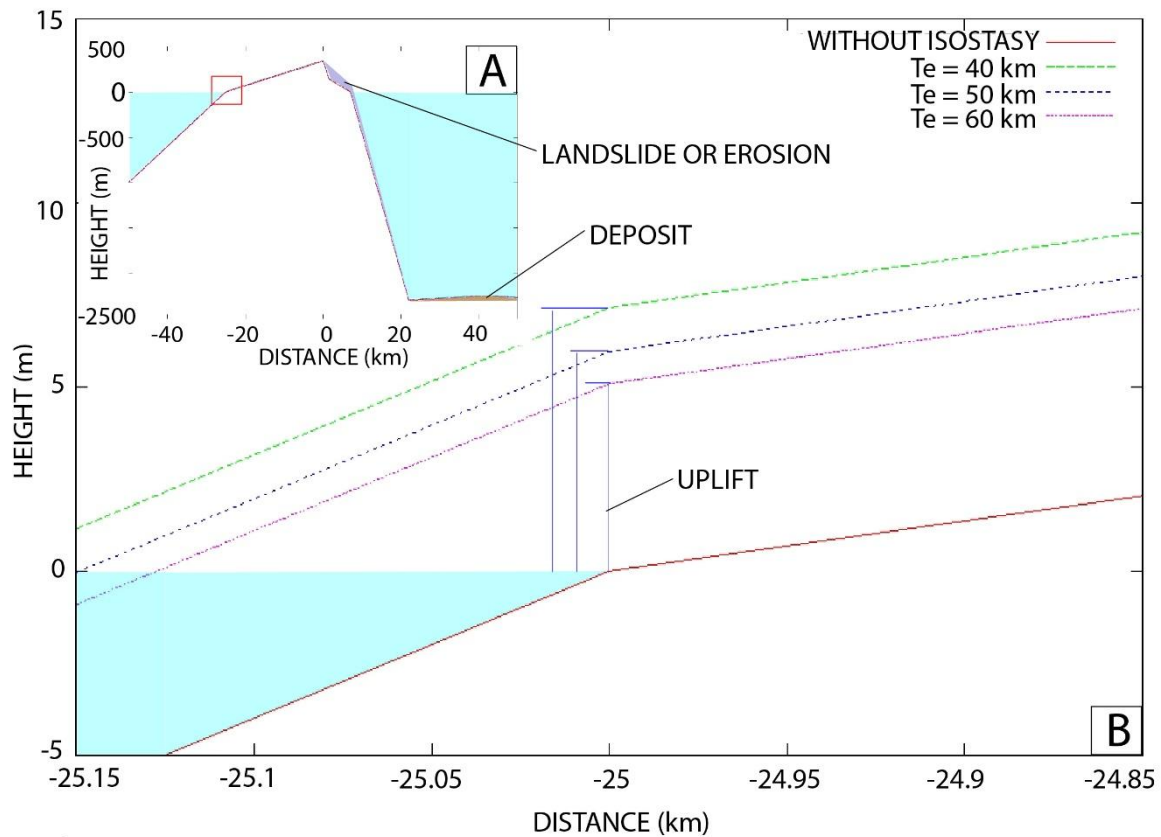


179

180 **Figure 5: Isostatic adjustment after an abrupt mass unloading of 10 km^3 . (A)**
 181 **Unloaded volume geometry, (B) Modelled uplift in the southwest part of the island after**
 182 **an abrupt mass unloading caused by an isostatic adjustment with elastic thicknesses of**
 183 **40 km, 50 km and 60 km.**

184 An uplift rate of 0.45 mm/yr in the southwest of Barbados, caused by an abrupt mass
 185 unloading of $30 \pm 10 \text{ km}^3$ in the northeast of Barbados, is estimated by modelling the
 186 Barbados lithosphere with an effective elastic thickness of $50 \pm 10 \text{ km}$ (Fig. 6C). Part of the
 187 abrupt mass unloading (20 km^3) occurred offshore. The increases of $0.45 \pm 0.15 \text{ mm/yr}$ after
 188 an abrupt mass unloading of $30 \pm 10 \text{ km}^3$ in the Scotland District explain the uplift rate
 189 increases observed in the Southwest coast of the Barbados from 0.34 to 0.8 mm/yr that
 190 occurred 11.2 kyr ago. The change in the uplift rate occurred in less than 0.2 kyr (Figure 3B).
 191 The accommodation of the uplift rate variation take place from 11.08 kyr to 11.28 kyr BP .

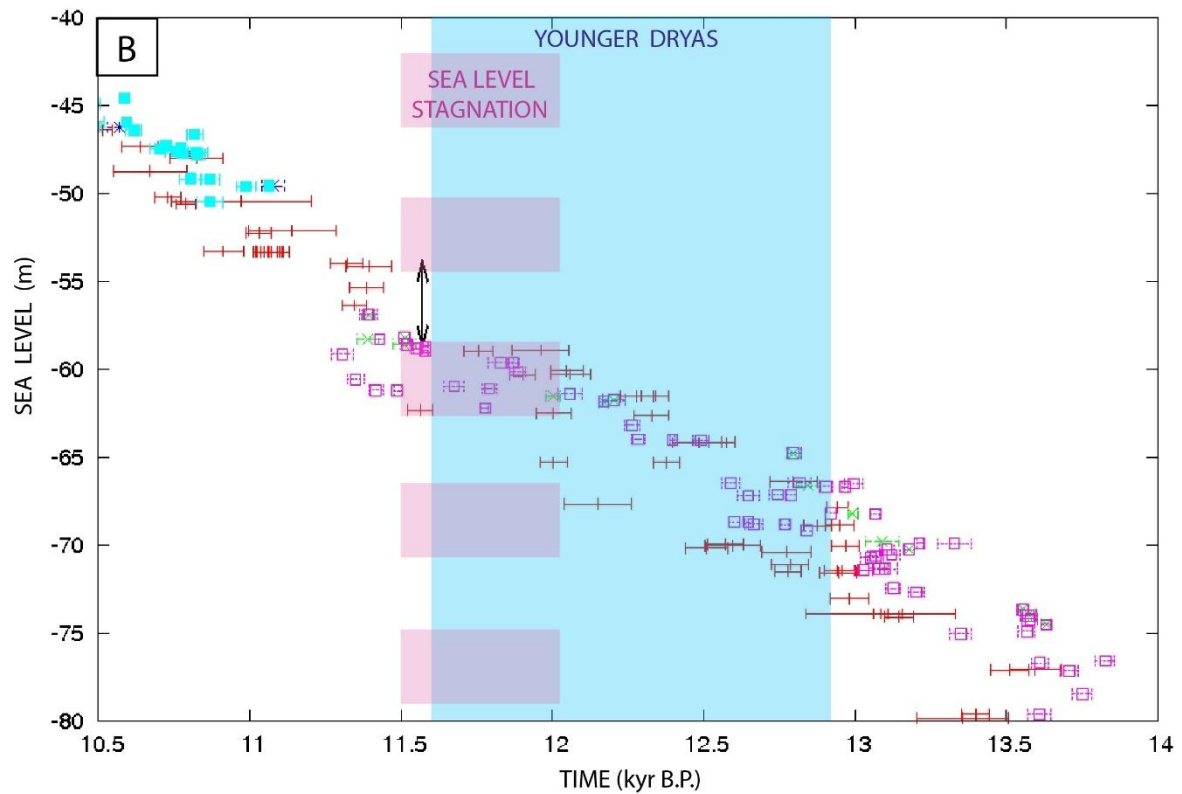
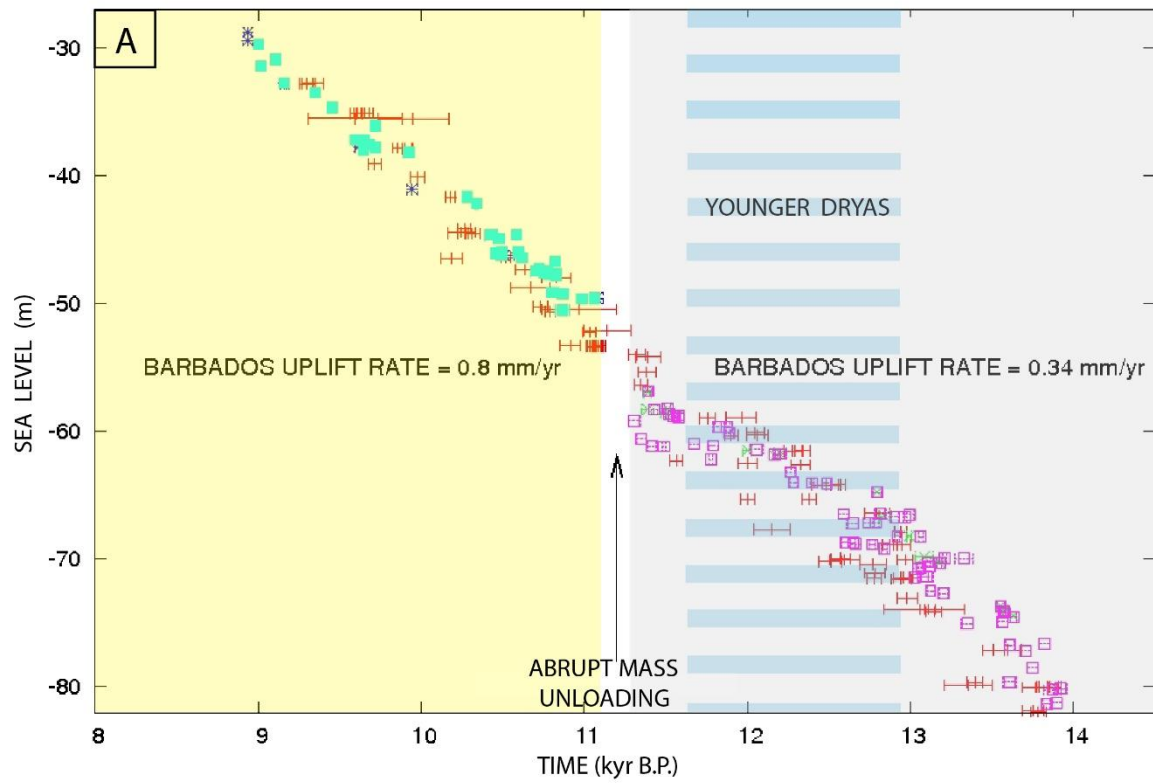
192



195 **FIGURE 6: Isostatic adjustment modelling. (A) Topography and bathymetry modelling**
196 **of Barbados Island before and after the abrupt mass unloading by erosion or landslides.**
197 **The red square represents the area near Bridgetown, where have been collected coral**
198 **reefs in previous studies at the Southwest of the Barbados and is detailed in Figure 1B.**
199 **(B) Modelling of the isostatic adjustment after an abrupt mass unloading of 50 km^3 for**
200 **different elastic thicknesses T_e with values of 40, 50 and 60 km. (C) Comparison of the**
201 **uplift rate caused by the isostatic adjustment triggered by abrupt mass unloading with**
202 **various volumes and for different elastic thickness. An abrupt unloading by a rock**
203 **volume of $20\text{-}40 \text{ km}^3$ causes an uplift rate of 0.45 mm/yr .**

204

205 This increase of uplift after 11.2 kyr permit to interpret the elevation of coral reefs from 14
206 kyr to 9 kyr in agreement with sea-level reconstruction from other areas. After reconstruction,
207 a rapid sea-level jump of 4.8 m is observed contemporaneously with Meltwater pulse 1B, 11.5
208 kyr ago, 150 yr after the end of the Younger Dryas (Fig. 7), and 300 yr before the abrupt mass
209 unloading. The sea-level jump was very short (i.e. $0.1 \pm 0.05 \text{ kyr}$). This represents a sea-level
210 rise of $65 \pm 35 \text{ mm/yr}$, whereas the mean sea-level rise from 14 to 9 kyr BP is of 10.4 mm/yr .



211

212 **FIGURE 7: Sea level variation with time. (A) Sea Level at different ages from Tahiti**
 213 **coral reefs data in red (Bar et al., 2010) corrected from a subsidence of 0.25 mm/yr and**
 214 **Barbados coral reefs data (Peltier and Fairbank, 2006; Abdul et al., 2016) with a**

215 correction of 0.8 mm/yr after 11.2 kyr in light blue (Abdul et al., 2016) and dark blue
216 (Peltier and Fairbank, 2006) and 0.34 mm/yr before 11.2 kyr in green (Peltier and
217 Fairbank, 2006) and pink (Abdul et al., 2016). (B) Sea-level reconstruction during the
218 period 13.5 to 10.5 kyr from coral reef with correction of uplift for Barbados (0.8 mm/yr
219 after 11.2 kyr and 0.34 mm/yr before 11.2 kyr) and subsidence for Tahiti (0.25 mm/yr).
220 Data from Peltier and Fairbank (2006) in green and dark blue, Bard et al. (2010) in red,
221 Abdul et al. (2016) in pink and light blue.

222

223 4 Discussion

224 4.1 Uplift rate variation with time

225 During the last thousand years, an uplift rate of 0.34 mm/yr was considered by
226 previous studies (Peltier and Fairbank, 2006; Abdul et al., 2016). From 14 to 11.2 kyr BP, the
227 0.34 mm/yr of uplift rate were caused by tectonic compression or diapirism [Speed, 1981,
228 Westerwood et al, 1988; Deville et al., 2006]. However, from 11.2 kyr to 9 kyr, an uplift rate
229 of 0.8 mm/yr explain the observed data, coherently with sea level variations used as a
230 reference. Sea level reference curve could be constructed using a tectonically stable area with
231 (intraplate) where coral samples have been collected following an homogeneous protocol and
232 accurately dated by U/Th method (Bard et al., 2010) or measuring the mean curve of
233 numerous studies using heterogeneous methods but with an accurate statistical approach
234 (Lambeck et al., 2014). If these curves converge for the last thousand years, they differ for
235 older ages and the last glacial period (>14.5 kyr BP). In this study, the curve obtained in
236 Tahiti Island (French Polunesia) using Bard et al. (2010) data is considered as a reference.

237 This uplift was partly (i.e. 0.45 mm/yr ; 56%) caused by the isostatic adjustment
238 related to an abrupt mass unloading in the northeast of Barbados. Isostatic adjustment could
239 explain the uplift increase during a short period of time (i.e. 10 kyr). Uplift changes during a
240 longer period (>> 10 kyr) cannot be explained by this process. It is not excluded that such
241 process may have played a role before the 11.2 kyr event, but this is beyond the scope of this
242 study.

243 Previous studies, considered that these different uplift rates were representative of two
244 distinct areas separated by a tectonic structure (Carlson and Clark, 2012; Bard et al., 2016).
245 Consequently, elevation of coral reefs of core 7, 13 and 15 in the southwest of Barbados were

246 criticized (Carlson and Clark, 2012) and Barbados sea-level reconstruction after 11.5 kyr BP
247 considered as not representative (Bard et al., 2016). Nevertheless, due to the older age of coral
248 reef located on core 7, 13 and 15 in comparison to the other data, it can be also considered
249 that a temporal variation of vertical movement occurred. Barbados coral reef can be used, as
250 those of Tahiti, to discuss sea-level variation during the last 14 kyr BP considering
251 appropriate uplift rates. An uplift rate of 0.8 mm/yr after 11.2 mm/yr provide coherent results
252 with previous sea-level reconstruction (Bard et al., 2010), uplift estimates (Carlson and Clark,
253 2012; Bard et al., 2016) and the cause of this uplift change is now explained.

254

255 4.2 Sea-level variation and climatic change

256 Sea-level rise from 14 to 9 kyr BP is almost constant at 10.4 mm/yr considering these
257 corrections (Figure 7), in agreement with previous studies in Tahiti, Barbados and Huon (Bard
258 et al., 2010). The main evolution during this period is between 12.0 and 11.5 kyr BP when a
259 stagnation of sea-level occurred at -60.5 ± 1.5 m. This sea-level perturbation is due to the
260 Younger Dryas cold event estimated to occur from the onset 12870 ± 30 yr BP to its
261 termination 11610 ± 40 yr BP (Cheng et al., 2020). At 11.5 kyr BP, around 150 yr after the
262 end of Younger Dryas, the present study shows that a rapid sea-level jump of 4.8 m occurred
263 in less than 0.1 ± 0.05 kyr representing a sea-level rise of 65 ± 35 mm/yr, faster than
264 previously estimated (i.e. 0.40 mm/yr; Abdul et al., 2016), contemporaneously with mi-
265 Atlantic discharge increase (Tarasoc and Peltier, 2005). This sea-level drop is smaller than
266 previously believed (i.e. 4.8 ± 1 m instead of value ranging from 7.5 ± 2.5 m to 14 ± 2 m;
267 Blanchon and Shaw, 1995; Fairbank, 1989; Abdul et al., 2016) and occurred before than
268 previous estimates (i.e. at 11.5 kyr BP instead of 11.45-11.1 kyr BP; Abdul et al., 2016), in
269 agreement with Lambeck et al. (2014). This sea-level jump is not an artifact due to tectonic
270 and isostatic adjustment, but was caused by ice sheet melting in response to North Atlantic
271 warming. Spatial variation of the uplift rate in Barbados between 14 and 9 kyr BP are not
272 necessary to interpret coral reef elevation, while applying temporal variation permit to obtain
273 coherent results between Tahiti and Barbados sea-level reconstruction. Higher uplift rate (i.e.
274 0.8 mm/yr) applied for correction of coral reef elevation that are older than 11.2 kyr BP
275 causes discrepancies with sea-level curve and are not justified.

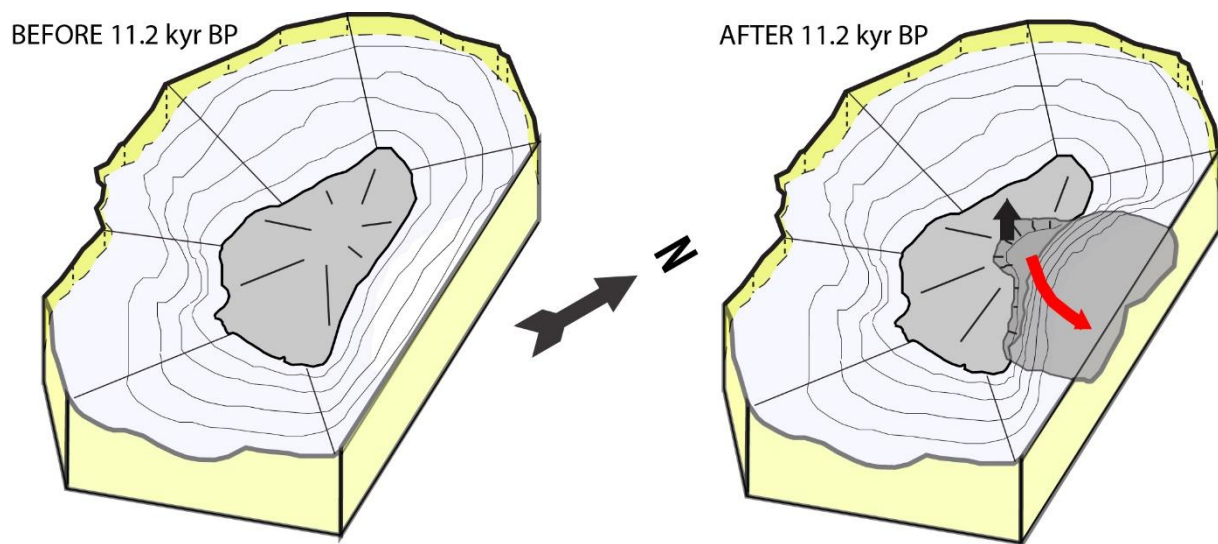
276 There is a delay between sea level drop and Younger Dryas cold event termination in
277 agreement with previous studies (Bard et al., 1996) that could be explained by thermal inertia

278 of large ice sheet and ocean dilatation. It was lagged by 150 yr instead of 400 yr (Abdul et al.,
279 2016) from Younger Dryas, but contemporaneously with meltwater megafloods from lake
280 Agassiz (Blanchon and Shaw, 1995; Smith et al., 1993) or Lena River (Tesi et al., 2016). The
281 main footprint of Younger Dryas on sea level is short (i.e. 0.5 kyr), but a slight reduction of
282 sea-level rise begun around 12.80 kyr BP.

283 4.3 Cause of abrupt mass unloading

284 The abrupt mass unloading occurred 0.3 kyr after rapid sea-level jump and 0.45 kyr
285 after the termination of Younger Dryas (Figure 8). At the termination of Younger Dryas,
286 climate warmed (Cheng et al., 2020) and became more humid. Sea-level increases and wetter
287 conditions are favorable to erosion and landslide (Brunetti et al., 2010; Urgeles and
288 Camerlinghi, 2013; Gargani et al., 2006; Gargani et al., 2014; Gargani, 2020). This event
289 occurred few time after the melting water pulse MWP-1B, contemporaneously with an
290 increase of the number of landslides (Owen et al., 2007; Smith et al., 2011). If associated with
291 erosion processes, the abrupt mass unloading of Barbados corresponds locally to a maximum
292 vertical erosion rate of ~ 1 m/yr and a regressive erosion rate of 37.5 ± 12.5 m/yr during 0.2
293 kyr, representing fast headcuts retreat in comparison to analog erosion processes (Gargani,
294 2004; Gargani et al., 2010; Vanmaercke et al., 2016).

295



296

297 **FIGURE 8: Schematic representation of the unloading process on geomorphology. Red**
298 **arrow represents landslide or erosion process. Black arrow represents uplift.**

299 **5 Conclusions**

300 Despite controversial results and continuous debate about the existence of meltwater
301 pulse 1B in sea level, our results suggests that it is not an artefact, but that the rapid sea-level
302 jump is smaller than previously estimated. Approximativly150 yr after the termination of
303 Younger Drias, a sea-level drop of 4.8 m occurred, contemporaneously with megaflood
304 events, after a short sea-level stagnation of 500 yr at -60.5 ± 1.5 m. An abrupt mass unloading
305 occurred 300 yr after the sea-level drop. The abrupt mass unloading (landslide or/and erosion)
306 occurred 11.2 kyr BP and caused isostatic adjustment. Isostatic adjustment, caused by an
307 abrupt mass unloading of $30 \pm 10 \text{ km}^3$ in less than 0.2 kyr, generates an uplift increase of 0.45
308 ± 0.15 mm/yr in Barbados. The uplift increase of 0.45 ± 0.15 mm/yr from 0.34 to 0.8 mm/yr
309 at 11.2 ± 0.1 kyr BP explain coral reef elevation in Barbados that were not fully coherent with
310 others sea level curves, previously to this study. Relative sea-level curves could be used to
311 detect abrupt mass unloading.

312 **Acknowledgments**

313 The author declare no competing interests.

314 **References**

315 Abdul N.A., Mortlock R.A., Wright J.D. & Fairbanks R.G. (2016), Younger Dryas sea level
316 and meltwater pulse 1B recorded in Barbados reef crest coral *Acropora palmata*.
317 *Paleoceanography*, v.31, p. 330-344

318 Austermann J., Mitrovica J.X., Latychev K. & Milne G.A. (2013), Barbados based estimate
319 of ice volume at Last Glacial Maximum affected by subducted plate. *Nat. Geoscience*, v.6, p.
320 553-537.

321 Bache F., Gargani J., Suc J-P., Gorini C., Rabineau M., Popescu S-M., Leroux E., Do Couto
322 D., Jouannic G., Rubino J-L., Olivet J-L., Clauzon G., Tadeu Dos Reis A. & Aslanian D.
323 (2015), Messinian evaportie deposition during sea level rise in the Gulf of Lions (Western
324 Mediterranean). *Marine and Petroleum Geology*, 66, 262-277.

325 Bard, E., Hamelin, B. & Fairbanks, R. (1990), U-Th ages obtained by mass spectrometry in
326 corals from Barbados: sea level during the past 130,000 years. *Nature*, 346, 456–458.

327 Bard, E., B. Hamelin, Fairbanks R.G. & Zindler, A. (1990b), Calibration of the 14C timescale
328 over the past 30,000 years using mass spectrometric U-Th ages from Barbados corals. *Nature*,
329 345, 405-410.

330

331 Bard E., Hamelin B., Arnold M., Montaggioni L., Cabiosh G., Faure G. & Rougerie F.
332 (1996), Deglacial sea-level record from Tahiti corals and the timing of global meltwater
333 discharge. *Nature*, 382, 241-244.

334

335 Bard E., Hamelin B. & Delanghe-Sabatier D. (2010), Deglacial Meltwater Pulse 1B and
336 Younger Dryas Sea Levels Revisited with Boreholes at Tahiti. *Science*.
337 10.1126/science.1180557.

338

339 Bard E., Hamelin B., Deschamps P. & Camoin G. (2016), Comment on « Younger Dryas sea
340 level and meltwater pulse 1B recorded in Barbados reefal crest coral *Acropora palmata* » by
341 N. A. Abdul et al., *Paleoceanography*, 31, 1603–1608.

342

343 Bender, M. L., Fairbanks, R. G., Taylor, F. W., Matthews, R. K., Goddard, J. G. & Broecker,
344 W. S. (1979), Uranium-series dating of the Pleistocene reef tracts of Barbados, West Indies.
345 *Geological Society of America Bulletin*, 90, 6, 577-594.

346

347 Blanchon P. & Shaw J. (1995), Reef drowning during the last deglaciation: evidence for
348 catastrophic sea-level rise and ice-sheet collapse. *Geology*, 23, 4-8.

349

350 Brunetti M. T., Peruccacci S., Rossi M., Luciani S., Valigi D. & Guzzetti, F. (2010), Rainfall
351 thresholds for the possible occurrence of landslides in Italy, *Nat. Hazards Earth Syst. Sci.*, 10,
352 447–458.

353

354 Camoin, G.F., Montaggioni L.F. & Braithwaite, CJR, (2004). Late Glacial to Post Glacial
355 Sea-Levels in the Western Indian Ocean. *Marine Geology*, 206: 119-146.

356

357 Carlson A. E. & Clark P.U. (2012), Ice sheet sources of sea level rise and freshwater
358 discharge during the last deglaciation, *Rev. Geophys.*, 50, RG4007.

359

360 Cheng H., Zhang H., Spötl C., Baker J., Sinha A., Li H., Bartolomé M., Moreno A., Kathayat
361 G., Zhao J., Dong X., Li Y., Ning Y., Jia X., Zong B., Ait Brahim Y., Pérez-Mejías C., Cai
362 Y., Novello V.F., Cruz F.W., Severinghaus J.P. & Lawrence Edwards Z.A.R. (2020), Timing
363 and structure of the Younger Dryas event and its underlying climate dynamics. *Proceedings of*
364 *the National Academy of Sciences*, 117, 38, 23408-23417.

365

366 Cruden D., Machel H.G., Knox J. . & Goddard R. (2014), The “Boscobel Landslip” of
367 October 1st, 1901 – the largest historic landslide in Barbados, West Indies. *Landslides*, 11,
368 673-684.

369

370 Deville E., Guerlais S-H., Callec Y., Gribouillard R., Huyghe P., Lallemand S., Mascle A.,
371 Noble M. & Schmitz J. (2006), Liquified vs. Stratified sediment mobilization processes:
372 Insight from the South of the Barbados accretionary prism. *Tectonophysics*, 428, 33-47.

373

374 Edwards T.L., Nowicki S., B. Marzeion, R. Hock, H. Goelzer, H. Seroussi, N.C. Jourdain,
375 D.A. Slater, F.E. Turner, C.M. McKenna, E. Simon, A. Abe-Ouchi, J.M. Gregory, E. Larour,
376 W.H. Lipscomb, A.J. Payne, A. Shepherd, C. Agosta, P. Alexander, T.A.B. Anderson, X.
377 Asay-Davis, A. Aschwanden, A. Barthel, A. Bliss, R. Calov, C. Chambers, N. Champollion,
378 Y. Choi, R. Cullather, J. Cuzzzone, C. Dumas, D. Felikson, X. Fettweis, K. Fujita, B.K.
379 Galton-Fenzi, R. Gladstone, N.R. Golledge, R. Greve, T. Hattermann, M.J. Hoffman, A.
380 Humbert, M. Huss, P. Huybrechts, W. Immerzeel, T. Kleiner, P. Kraaijenbrink, S. Le clec’h,
381 V. Lee, G.R. Leguy, C.M. Little, D.P. Lowry, J-H. Malles, D.F. Martin, F. Maussion, M.
382 Morlighem, J.F. O’Neill, I. Nias, F. Pattyn, T. Pelle, S.F. Price, A. Quiquet, V. Radić, R.

383 Reese, D.R. Rounce, M. Rückamp, A. Sakai, C. Shafer, N-J. Schlegel, S. Shannon, R.S.
384 Smith, F. Straneo, S. Sun, L. Tarasov, L.D. Trusel, J. Van Breedam, R. van de Wal, M. van
385 den Broeke, R. Winkelmann, H. Zekollari, C. Zhao, T. Zhang & T. Zwinger (2021), Projected
386 land ice contributions to twenty-first-century sea level rise. *Nature* **593**, 74–82 (2021).
387 <https://doi.org/10.1038/s41586-021-03302-y>

388

389 Fairbank R.G. (1989), A 17000-year glacio-eustatic sea level record: influence of glacial
390 melting rates on the Younger Dryas event and deep-ocean circulation. *Nature*, 342, 637-642.

391

392 Gallup C.D., Edward R.L. & Johnson R.D. (1994), The Timing of high sea levels over the
393 past 200 000 years. *Science*, 263, 782-786.

394

395 Gargani, J. (2004), Modelling of the erosion in the Rhone valley during the Messinian crisis
396 (France), *Quaternary International*, 121, 13-22.

397

398 Gargani J., Stab O., Cojan I. & Brulhet J. (2006), Modelling the long-term fluvial erosion of
399 the River Somme during the mast million years. *Terra Nova*, 18, 115-129.

400

401 Gargani, J. & Rigollet C. (2007), Mediterranean Sea level variations during the Messinian
402 Salinity Crisis. *Geophysical Research Letters*, vol.34, L10405.

403

404 Gargani J., Rigollet C. & Scarselli S. (2010), Istostatic response and geomorphological
405 evolution of the Nile valley during the Messinian salinity crisis, *Bulletin Soc. Geol. France*,
406 181, 19-26.

407

408 Gargani J., Bache F., Jouannic G. & Gorini C. (2014), Slope destabilization during the
409 Messinian Salinity Crisis. *Geomorphology*, 213, 128-138.

410

411 Gargani J. (2020), Modelling the mobility and dynamics of a large Tahitian landslide using
412 runout distance. *Geomorphology*, 370, 107354.

413

414 Haq B.U., Schutter S.R., (2008). A chronology of Paleozoic Sea-Level Changes. *Science*,
415 v.322, n.5898, 64-68.

416

417 Hoojer A. & Vernimmen R. (2021), Global LIDAR land elevation data reveal greatest sea-
418 level rise vulnerability in the tropics. *Nature Communications*, 12, 3592.

419

420 Jiménez-Díaz A., Ruiz J., Pérez-Gussinyé M., Kirby J.F., Álvarez-Gómez J.A., Tejero R. &
421 Capote R. (2014), Spatial variations of effective elastic thickness of the lithosphere in Central
422 America and surrounding regions. *Earth and Planetary Science Letters*, v.391.

423

424 Lambeck K., Rouby H., Purcell A., Sun Y. & Sambridge M. (2014), Sea level and global ice
425 volumes from the Last Glacial Maximum to the Holocene. *Proceedings of the National
426 Academy of Sciences*, v. 111, 43, 15296–15303.

427

428 Mesoellea, K.J. (1967), Zonation of Uplifted Pleistocene Coral Reefs on Barbados, West
429 Indies. *Science*, 156, 638-640.

430

431 Mesoellea K. J., Matthews R. K., Broecker W. S. & Thurber D. L. (1969), The Astronomical
432 Theory of Climatic Change: Barbados Data. *The Journal of Geology*, 77, 3, 250-274.

433

434 Mitrovica, J. X., Forte, A. M., & Simons, M. (2000), A reappraisal of postglacial decay times
435 from Richmond Gulf and James Bay, Canada. *Geophys. J. Int.*, 142(3), 783-800.

436

437 Owen M., Day S., Maslin M. (2007), Late Pleistocene submarine mass movements:
438 occurrence and causes. *Quaternary Science Reviews*, 26, 958-978.

439

440 Pedoja K., Husson L., Johnson M.E., Melnick D., Witt C., Pochat S., Nexer M., Delcailleau
441 B., Pinegina T., Poprawski Y., Authemayou C., Elliot M., Regard V., Garestier F., (2014).
442 Coastal staircase sequences reflecting sea-level oscillations and tectonic uplift during the
443 Quaternary and Neogene. *Earth-Science Reviews*, 132, 13-38.

444

445 Peltier W.R. & Fairbank R.G. (2006), Global glacial ice volume and last glacial maximum
446 from extended Barbados sea level record. *Quaternary Science review*, 25, 3322-3337.

447

448 Pichot T., Lafuerza S., Patriat M. & Roest W. (2016), Pleistocene Mass Transport Deposits
449 Off Barbados Accretionary Prism (Lesser Antilles). In *Submarine Mass Movements and their*
450 *Consequences*, Volume 41 of the series *Advances in Natural and Technological Hazards*
451 *Research*, 321-329.

452

453 Prior D. B. & Ho C. (1972), Coastal *and* mountain slope instability *on the* islands of St. Lucia
454 *and* Barbados. *Eng. Geol.*, 6, 1-18.

455

456 Radtke U. & Schellmann G. (2006), Uplift History along the Clermont Nose Traverse on the
457 West Coast of Barbados during the Last 500,000 Years — Implications for Paleo–Sea Level
458 Reconstructions. *Journal of Coastal Research*, 22, 2, 350-356.

459

460 Regard V., Prémaillon M., Dewez T.J.B., Carretier S., Jeandel C., Godderis Y., Bonnet S.,
461 Schott J., Pedoja K., Martinod J., Viers J., S. Fabre S. (2022). Rock coast erosion : an
462 overlooked source of sediments to the ocean. Europe as an example. *Earth and Planetary*
463 *Science Letter*, v.579, 117356.

464

465 Smith D.G. & Fisher T.G. (1993), Glacial Lake Agassiz: The northwestern outlet and
466 paleoflood. *Geology*, 21 9-12.

467

468 Smith, J. R. & Wessel, P. (2000), Isostatic consequences of giant landslides on the Hawaiian
469 ridge. *Pure and applied geophysics*, 157, 1097-1114.

470

471 Smith D.E., Harrison S., Firth C.R. & Jordan J.T. (2011), The early Holocene sea level rise.
472 *Quaternary Science Reviews*, 30, 1846-1860.

473

474 Speed R.C. (1981), Geology of Barbados: implications for an accretionary origin.
475 *Oceanologica Acta*. 259-265.

476

477 Tarasov L. & Peltier W.R. (2005), Artic freshwater forcing of the Younger Dryas cold
478 reversal. *Nature*, 435, 662-665.

479

480 Tesi, T., Muschitiello F., Smittenberg R.H., Jakobsson M., Vonk J.E., Hill P., Andersson A.,
481 Kirchner N., Noormets R., Dudarev O., Semiletov I. & Gustafsson Ö. (2016), Massive
482 remobilization of permafrost carbon during post-glacial warming. *Nat. Commun.* **7**, 13653.

483

484 Turcotte, D. L., & Schubert, G. (2001), *Geodynamics*, 2nd ed., 456 pp., Cambridge Univ.
485 Press, New York.

486

487 Urgeles R. & Camerlinghi A. (2013), Submarine landslides of the Mediterranean Sea:
488 Trigger mechanisms, dynamics, and frequency-magnitude distribution. *Journal of*
489 *Geophysical Research*, 118, 2600-2618.

490

491 Van der Wal, W., Wu, P., Wang, H., & Sideris M. G. (2010), Sea levels and uplift rate from
492 composite rheology in glacial isostatic adjustment modelling. *Journal of Geodynamics*, 50,
493 38-48.

494

495 Vanmaercke M., Poesen J., Van Mele B., Demuzere M., Bruynseels A., Golosov V.,
496 Rodrigues Bezerra J.F., Bolysov S., Dvinskih A., Frankl A., Fuseina Y., Teixeira Guerra A.J.,
497 Haregeweyn N., Ionita I., Imwangana F.M. Moeyersons J., Moshe I., Samani A.N., Niascu L.,
498 Nyssen J., Otsuki Y., Rdoane M., Rysin I., Ryzhov Y.V. & Yermolaev O. (2016), How fast
499 do gully headcuts retreat? *Earth-Science Reviews*, 154, 336-355.

500

501 Westbrook G.K., Lass J.W., Buhl P., Bangs N., Tiley G.J. (1988), Cross section of an
502 accretionary wedge: Barbados ridge complex. *Geology*, 16, 631-635.

503

504 Zinke J, Reijmer JJG, Thomassin BA, Dullo WChr, Grootes PM, Erlenkeuser H (2003).
505 Postglacial flooding history of Mayotte lagoon (Comoro Archipelago, southwest Indian
506 Ocean). *Mar Geol* 194:181–196.

507